SUPPLEMENTAL INFORMATION

Supplemental Experimental Procedures

Fly strains and husbandry

Fly stocks were raised using standard Bloomington medium at 18°C, 25°C, or 29°C as noted. The following fly stocks were used: *hs-flp* on the X chromosome (Bloomington Stock Center BL-26902), *nos-Gal4* on the 2nd chromosome (Van Doren et al., 1998), *UASp-FRT-H3-GFP-PolyA-H3-mKO* on the 3rd chromosome, *UASp-FRT-H3.3-GFP-PolyA-H3.3-mKO* on the 3rd chromosome, and *UASp-FRT-H2B-GFP-PolyA-H2B-mKO* were reported previously (Tran et al., 2012). Other new histone transgenic strains generated for this work are described as following and are all on either the 2nd or the 3rd chromosome as a single-copy transgene.

Generation of fly strains with different switchable dual-color transgenes

Standard procedures were used for all molecular cloning experiments. Enzymes used for plasmid construction were obtained from New England Biolabs (Beverly, MA). The new histone sequences as *histone-mKO*, *histone-mCherry*, or *histone-PAmCherry* fusion sequences were recovered as an XbaI flanked fragment and were subsequently inserted into the XbaI site of the UASp plasmid to construct the *UASp-new histone* plasmid. The old histone sequences as *histone-GFP*, *histone-EGFP*, or *histone-Dronpa* fusion sequences were inserted to *pBluescript-FRT-NheI-SV40 PolyA-FRT* plasmid at the unique NheI site. The entire *NotI-FRT-old histone-SV40 PolyA-FRT-EcoRI* sequences were then subcloned into the *UASp-new histone* plasmid digested by *NotI* and *EcoRI*. The final *UASp-FRT-old histone-PolyA-FRT-new histone* plasmids were introduced to w^{1118} flies by P-element-mediated germline transformation (Bestgene Inc.). Transgenic flies with the following transgenes were newly generated in studies reported here:

UASp-FRT-H4-GFP-PolyA-FRT-H4-mKO, *UASp-FRT-H4-EGFP-PolyA-FRT-H4-mCherry*, *UASp-FRT-H2A-GFP-PolyA-FRT-H2A-mKO*, *UASp-FRT-H2A-EGFP-PolyA-FRT-H2A-mCherry*, *UASp-FRT-H1-GFP-PolyA-FRT-H1-mKO*, *UASp-FRT-H3-Dronpa-PolyA-FRT-H3-PAmCherry*, and *UASp-FRT-H3.3-Dronpa-PolyA-FRT-H3.3-PAmCherry*.

Generating knock-in fly strains to tag genes encoding key DNA replication components

In collaboration with Fungene Inc. (Beijing, China), the following fly lines were generated using the CRISPR-Cas9 technology: CG6768 (DNA polymerase ε 255kD subunit) with 3HA tag at the 3' immediately upstream of the STOP codon, in order to generate the following fusion protein: DNA Polε-3HA; CG5602 (DNA ligase I, major replicative ligase) with 3HA tag at the 3' immediately upstream of the STOP codon, in order to generate the following fusion protein: DNA ligase-3HA.

Heat shock scheme

Flies with *UASp*-dual color histone transgenes were paired with *nos-Gal4* drivers. Flies were raised at 25°C throughout development until adulthood to avoid pre-flip.

For adult males: Before heat shock, 0-3 day old males were transferred to vials that had been air dried for 24 hours. Vials were submerged underneath water up to the plug in a circulating 37°C water bath for 90 minutes and recovered in a 29°C incubator for indicated time before dissection, followed by immunostaining or live cell imaging experiments.

For wandering third-instar larvae: bottles containing third instar larvae (pre-wandering stage) were submerged underneath water up to the plug in a circulating 37°C water bath for 90 minutes

and recovered in a 29°C incubator for indicated time before dissection, followed by fiber preparation and immunostaining experiments.

Immunostaining experiments

Immunofluorescence staining was performed using standard procedures (Hime et al., 1996; Tran et al., 2012). Primary antibodies were mouse anti-Fas III (1:200, DSHB, 7G10), anti-HA (1:200; Sigma-Aldrich H3663), anti-PCNA (1:200; Santa Cruz sc-56), anti-GFP (1:1,000; Abcam ab 13970), anti-mKO (1:200; MBL PM051M), and anti-BrdU (1:200; Abcam ab6326). BrdU analogue was Invitrogen B23151 5-bromo-2´-deoxyuridine (BrdU). Secondary antibodies were the Alexa Fluor-conjugated series (1:1000; Molecular Probes). Images for immunostained fixed sample were taken using Zeiss LSM 700 Multiphoton confocal microscope with 63x or 100x oil immersion objectives and processed using Adobe Photoshop software.

EdU incorporation to label GSC-GB pair at S-phase

To avoid quantifying cells which become arrested and fail to progress throughout the cell cycle following heat shock, we utilized EdU, a thymidine analogue which can label cells actively undergoing DNA replication in post-mitotic GSC-GB pairs. EdU labeling of the GSC-GB pairs at S phase was performed using Click-iT EdU Alexa Fluor 647 Imaging Kit (Life Science C10640) according to manufacturer's instructions. Dissected testes were immediately incubated in S2 medium with 100 μM EdU for 30 minutes at room temperature. The testes were subsequently fixed and proceed to primary antibody incubation. Fluorophore conjugation to EdU was performed along manufacturer's instructions and followed by secondary antibodies incubation.

Quantification of GFP and mKO intensity in whole testis

No antibody was added to enhance either GFP or mKO signal. Values of GFP and mKO intensity were calculated using Image J software: DAPI signal was used to determine the area of nucleus for measuring both GFP and mKO fluorescent signals, the raw reading was subsequently adjusted by subtracting fluorescence signals in the hub region used as background in both GSC and GB nuclei and compared between each other.

Live cell imaging

For live-cell imaging, adult *Drosophila* testes were dissected in a live cell imaging medium: Schneider's medium containing 200 μg/ml insulin, 15% (vol/vol) FBS, 0.6x pen/strep, pH ~7.0. Testes were then placed on a Poly-D-lysine coated FluoroDish (World Precision Instrument, Inc.) contain live cell imaging medium. All live-cell imaging was performed on spinning disc confocal microscope (Zeiss) equipped with an evolve^{-TM} camera (Photometrics), using a 63x Zeiss objective (1.4 NA). ZEN 2 software (Zeiss) was used for acquisition with 2x2 binning. Mitotic cells were used to reconstruct 3D videos using Imaris software (Bitplane), and the videos were shown in Supplementary Movie S1- S6.

The 3D histone quantification from time-lapse movie

The 3D histone quantification was done on telophase GSCs and spermatogonial cells (SGs, 8-cell cyst) using the time lapse movies. Quantification of histone signal on telophase cells was done manually: In brief, un-deconvolved 2D Z-stacks were saved as un-scaled 16-bit TIF images and the sum of the gray values of the pixels in the image ("RawIntDen") were determined using

Fiji software (Image J). A circle was drawn around histones (marked by EGFP or mCherry), and an identical circle was drawn in the hub region (background). The sum of the histone of each individual Z-stack was calculated by subtracting the sum of the gray values of the pixels of the background from the sum of the gray values of the pixels of the histone. The total amount of histone in the nuclei was calculated by adding the gray values of the signals from all Z-stacks.

Two color PALM imaging

For two color PALM imaging, 0-3 day old *UASp-FRT-H3-Dronpa-PolyA-FRT-H3-PAmCherry* and *UASp-FRT-H3.3-Dronpa-PolyA-FRT-H3.3-PAmCherry* flies were heat shocked using the heat-shock protocol specified previously. Flies were recovered 10-14 hours and then dissected for testis samples, which were immunostained with anti-Fas III primary antibody (1:200, DSHB, 7G10) overnight at 4˚C. Testes were then washed and subsequently incubated with AlexaFluo700 (1:2,000) secondary antibody to label the hub. After immunostaining, testes were washed, mounted on a glass slide and sandwiched between a glass slide and #1 cover glass with 8-10 µL PBS buffer. All PALM image acquisitions were performed on an Olympus IX-81 inverted microscope with a 1.45 NA 100 X TIRF objective and a ZT405/488/561/647rpc dichroic mirror (Chroma) as descried in (Buss et al., 2015). OptoSplit III (89 North) containing two dichroic mirrors (T556lpxr and T647lpxr, Chroma) was set between the microscope and an Andor Ultra 888 EmCCD camera to split signal from different fluorophore. Three emission filters, ET525/50, ET605/75, and ET700/75 (Chroma) were used for the Dronpa, PAmCherry, and AlexaFluor700 channel, respectively. Coherent 488nm, 561nm, and 647nm OBIS lasers

were chosen to excite the corresponding fluorophore. Another 405nm OBIS laser was combined for photo-activation or photo-switching of Dronpa and PAmCherry, respectively.

The imaging was preformed sequentially to prevent background from crosstalk between different channels. The samples were first scanned in Z axis every 1 μm using low 647nm power (15W/cm^2) to determine the position of the hub. Then the focal plane was fixed on a certain Z position with good and clear FasIII signal labeling hub cells. A high 647nm power (300W/cm^2) was then applied for ~2 min to bleach the signal from AlexaFluor700, which could significantly decrease the background in the shorter wavelength channels. Three or four 1500-frame acquisitions of Dronpa signal were then obtained with a 30 frame/second rate at 250 W/cm^2 488nm laser power. A 3-second 405 nm laser (1.5 W/cm^2) pulse was inserted between two consecutive acquisitions to convert Dronpa from the dark state to the fluorescent state. We exhausted most of the Dronpa signal during the imaging. And three or four 2000-frame acquisitions of PAmCherry were obtained at the same rate at 800 W/cm^2 561nm laser power. We kept the 405nm laser illumination during PAmCherry imaging but ramped up the power with an increment of 4.5 W/cm^2.

For two-color registration with superresolution, we imaged multi-colored emission TetraSpeck beads (100 nm diameter, ThermoFisher), as described previously (Hensel et al., 2013). In brief, we took snapshots of single TetraSpeck beads at different X-Y position (by ASI stage, MS-2000) in both Dronpa and PAmCherry channels. After PALM data processing (see below), a set of coordinates pairs were generated as control points. We then calculated the geometric transformation of the ‘PAmCherry coordinates’ to the ‘Dronpa coordinates’ using the '

fitgeotrans' function with the 2nd order polynomial method in MATLAB 2017a. The registration error in our system is about ~12-nm calculated from TetraSpeck bead samples.

Two-color PALM data processing

The Dronpa channel images were first filtered by a temporal median filter (Hoogendoorn et al., 2014) with a 201-frame time window to reduce the uniform background of the tissue sample. Then the coordinate of each individual Dronpa/PAmCherry spot was fitted by a 2D-Gaussian model using an ImageJ based plugin, ThunderSTORM (Ovesny et al., 2014). We chose the threshold of spot detection as 1.2 or 1.5*std (Wave.F1) for Dronpa and PAmCherry, respectively. The coordinates with small (< 0.5*mean) or large (> 3*mean) sigma and intensity were subsequently removed to prevent single-pixel noise or big molecule chunks. The localization uncertainty was calculated to be ~ 60 in Dronpa channel and ~40nm in PAmCherry channel.

GSCs were then cropped out based on the hub position, and PAmCherry coordinates were first calibrated by transformation using the matrix generated from TetraBead. To measure the degree of co-localization, we applied pairwise cross-correlation method established in (Veatch et al., 2012). We have shown the mean pairwise cross-correlation function (PCCF) is not affected by the blinking caused over-counting or low-labeling caused under-sampling (Coltharp et al., 2014). Therefore, we calculated the PCCF for individual cells and normalized by its own spot density (Veatch et al., 2012). The overall PCCF were averaged from all the GSCs collected.

Random simulation was performed on each cell. We generated Dronpa and PAmCherry spots with the same number of the experiment. The spots randomly distributed in the cell area. PCCF of each simulated cell was calculated in the same way as the experimental data set.

STORM imaging

EdU pulse-labeled DNA fibers were prepared on cover slides and clicked as described previously using the Alexa Fluoro 647 Click-it kit (Thermo Fisher Scientific). 10μL STORM buffer containing 10mM MEA (Dempsey et al., 2011) was used for imaging on the same microscope described in 2-color PALM imaging. 1kW/cm2 647nm laser was applied for single Alexa Fluoro 647 imaging. 20 – 40 movies with 3000 frames (33 frames/second) were collected for each STORM image. We also applied a low power 405nm laser illumination (1 W/cm^2) during imaging to reactivate the fluorophores in dark state. The reconstruction of STORM image was processed in a similar way as the PALM in ImageJ plugin ThunderSTORM with a higher detection threshold 2*std (Wave.F1). The spots located closer than the resolution (~16 nm) and within 5 frames were merged to recalculate the position. The drifting was calibrated by a standard cross-correlation method incorporated in the plugin.

STED fiber quantification analysis:

To capture localized asymmetries on chromatin fibers, fibers were divided into 2μm segments along the length of both sister fibers. Two microns was chosen due to the fact that this was the

average size of individual replicons in 10 minute EdU pulses (Figure S5). Assuming a DNA polymerase rate of 1kb/min, these regions likely represent ~10kb of DNA. Furthermore, due to inconsistencies in protein retention and antibody labelling during sample preparation, fluorescence signal strength showed a high degree of variability across fiber preparations. Therefore, in order to effectively compare histone distribution patterns across multiple sets of doublet fiber segments, we normalized fiber data using the following strategy to obtain ratio between the two sisters: First, we quantified fluorescence levels for both old histone (GFP) and new histone (mKO) for each singlet fiber segment making up the doublet fiber segment. We then divided the singlet fiber segment with greater fluorescence intensity by the singlet fiber segment with less fluorescence intensity to generate a ratio of the relative difference in histone enrichment levels.

Supplementary Figures and Figure Legends:

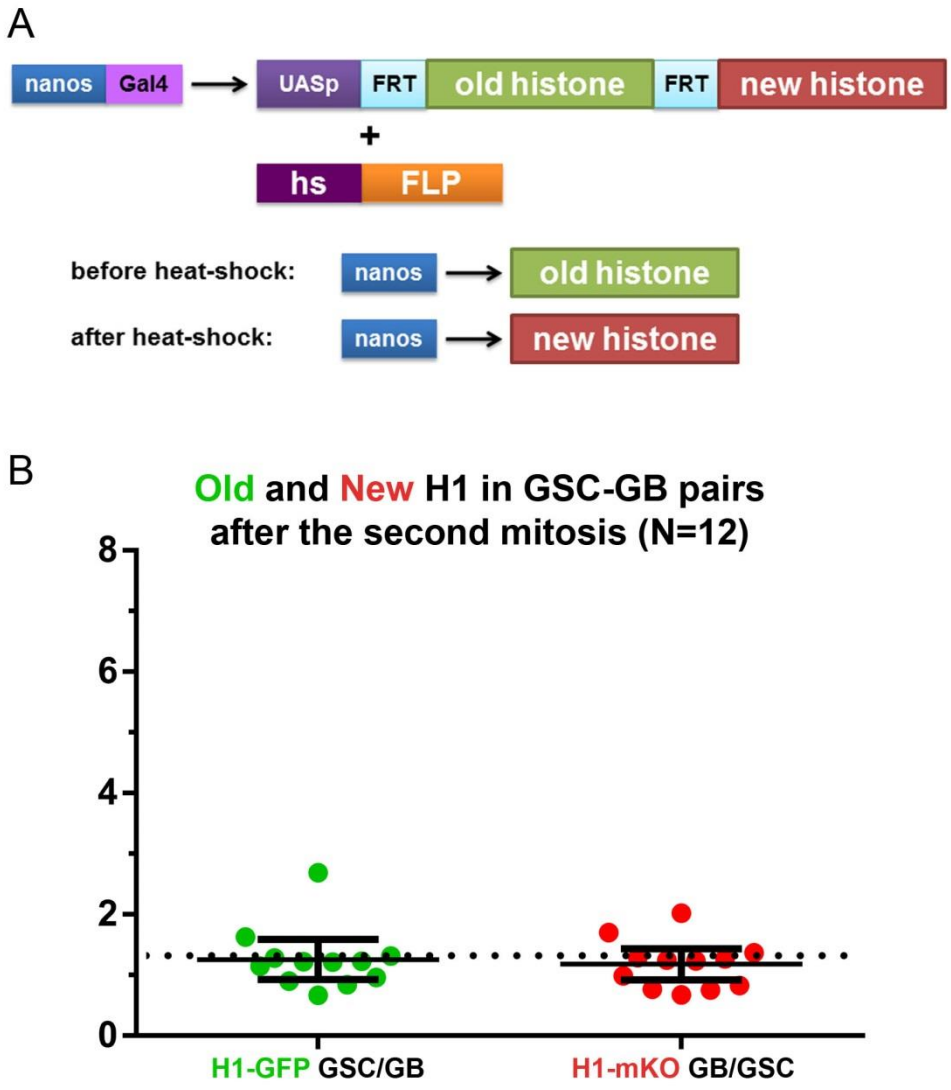

Figure S1: (**A**) A schematic diagram showing the dual color switch design that expresses pre-existing histone and newly synthesized histone by heat-shock treatment, as adapted from (Tran et al., 2012). (**B**) Histone H1 showed symmetric inheritance pattern in post-mitotic GSC-GB pairs (n= 12).

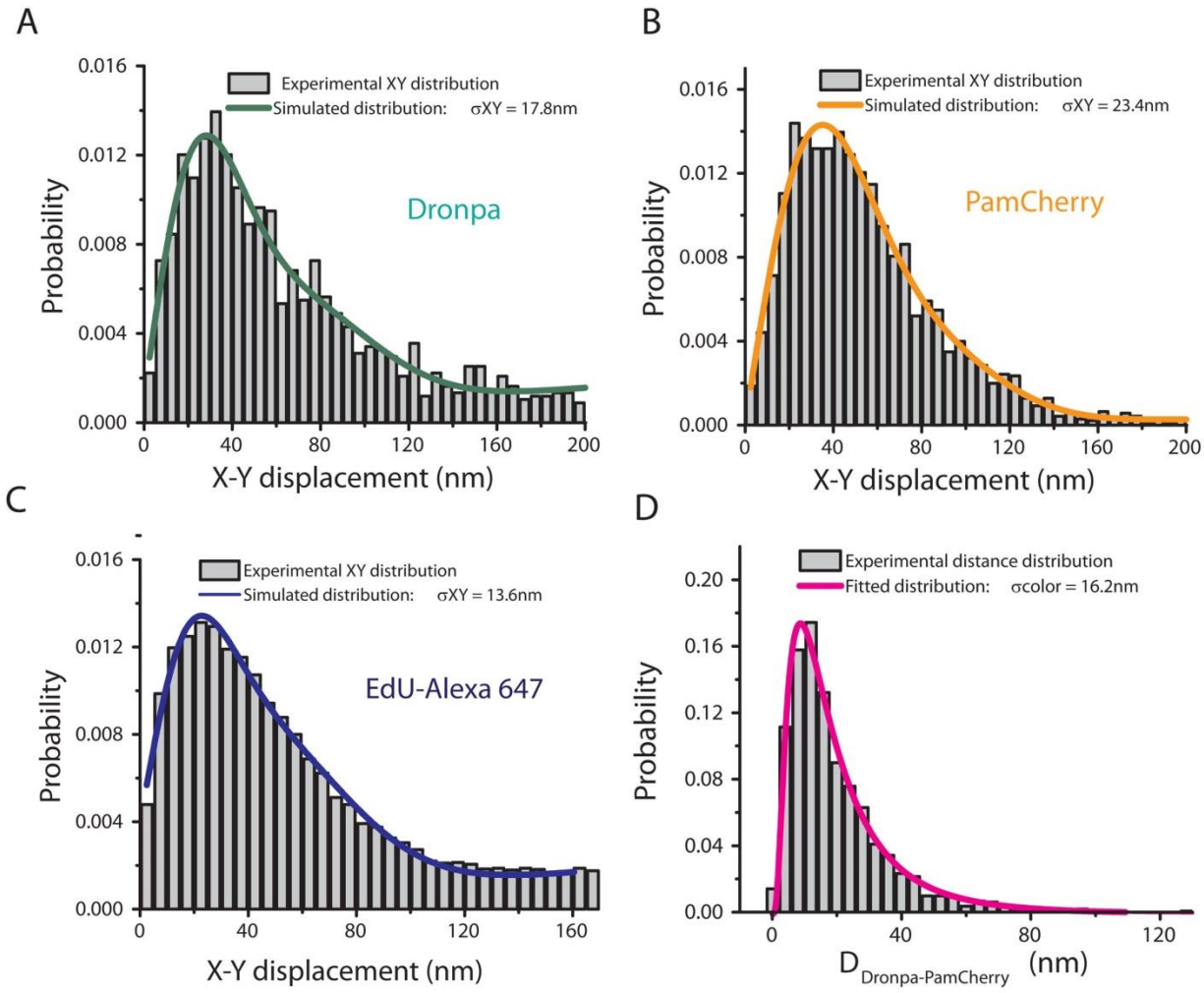

Figure S2: Localization precision measurement. (**A**) The pair-wise distance distribution of single Dronpa molecules in consecutive frames was calculated and fitted as previous described (Coltharp et al., 2016). (**B**) and (**C**) The average precision was estimated as 17.8nm. (**D**) The average precision of PAmCherry and EdU-Alexa Fluor 647 were calculated to be 23.4 nm and 13.6 nm in the same way. The registration error of two-color PALM was measured by calculating the deviation of the position of single TetraSpeck bead in different color channels. The distribution was fitted by a log-normal peak which gave an average error of 16.2 nm. See **Table S6**.

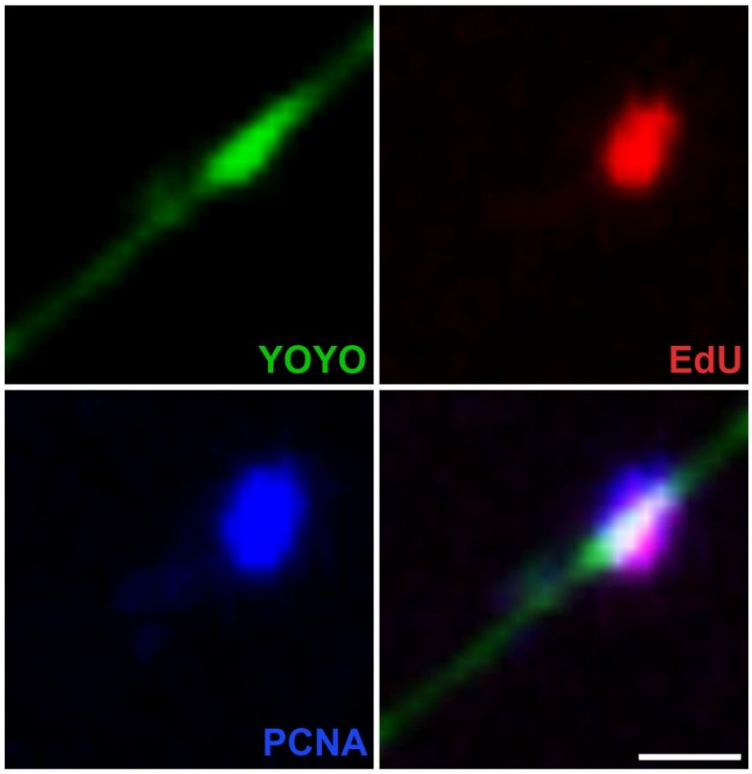

Figure S3: Chromatin fiber stained with YOYO-3 (green), anti-PCNA (blue) and pulsed with EdU (red). This image was taken using confocal microscopy. Scale bar: 1μm.

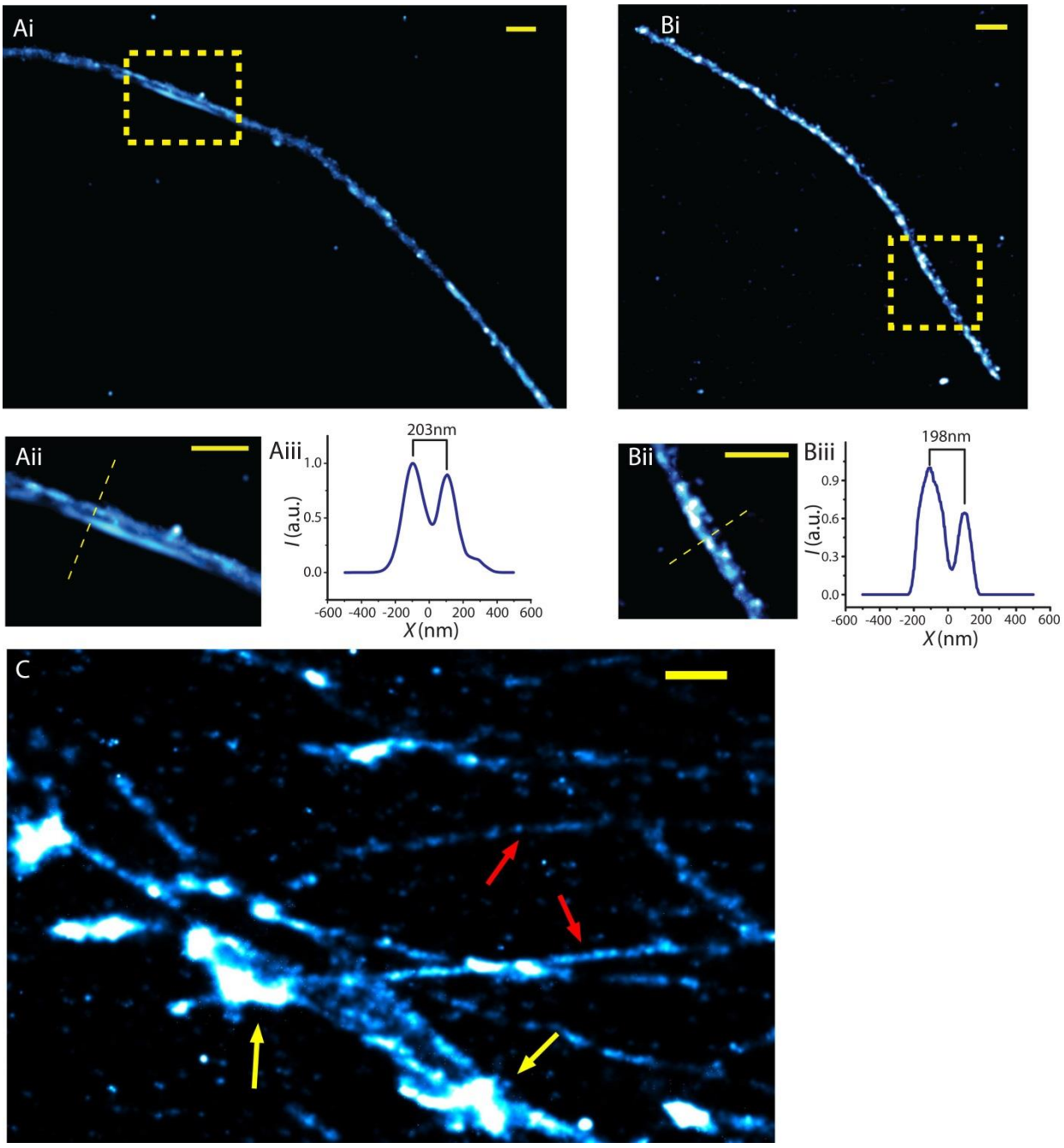

Figure S4: STORM image of EdU pulse-labeled chromatin fibers. (**Ai**) (**Bi**) Two representative STORM images of sister chromatids: The sister chromatids could be distinguished in the boxed regions where the two fibers have a breathing region, shown as zoomed-in images in (**Aii**) and (**Bii**), respectively. A line scan of the two strands (dash lines) was shown in (**Aiii**) and (**Biii**). The two sister chromatids are separated in ~ 200nm, similar to STED images shown

in Figure 4 and Figure 7, with a FWHM of ~ 100nm. Both the distance in between sisters and the width of each one of the two sisters are significantly larger than the STORM resolution (13.6nm, Figure **S2C**). (**C**) An example of chromatin fiber bundles pointed by yellow arrows. Red arrows point to unbundled fibers. Scale bars: 1μm.

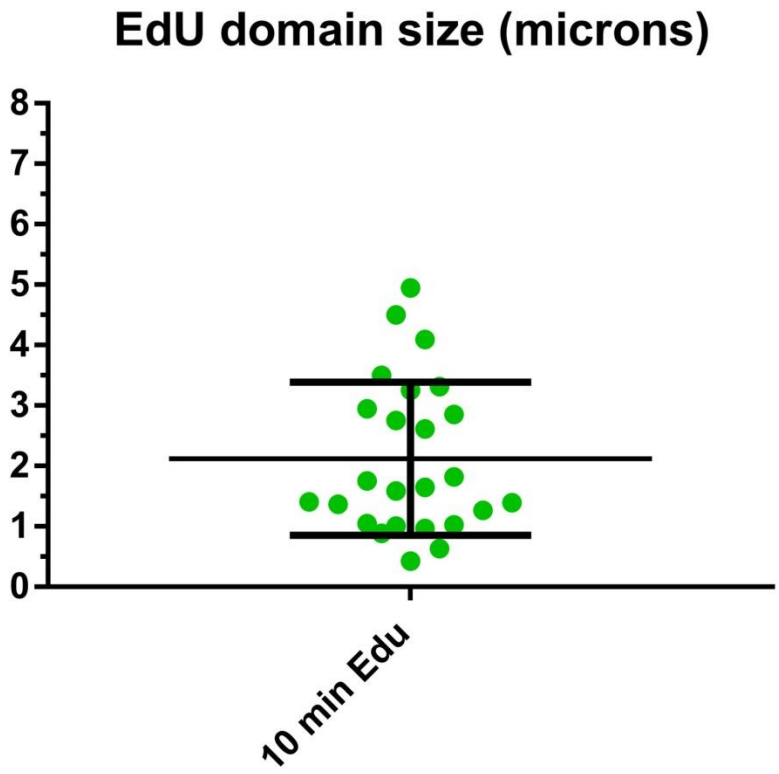

Figure S5: Size of chromatin fiber pulsed with 10-minute EdU. The 10 minute EdU-pulse is the shortest one that we could get EdU signal on fibers, which yields on average 2μm-long chromatin fiber. Assuming a DNA polymerase rate of 1kb per min, a 2um stretch on fiber ~ 10kb.

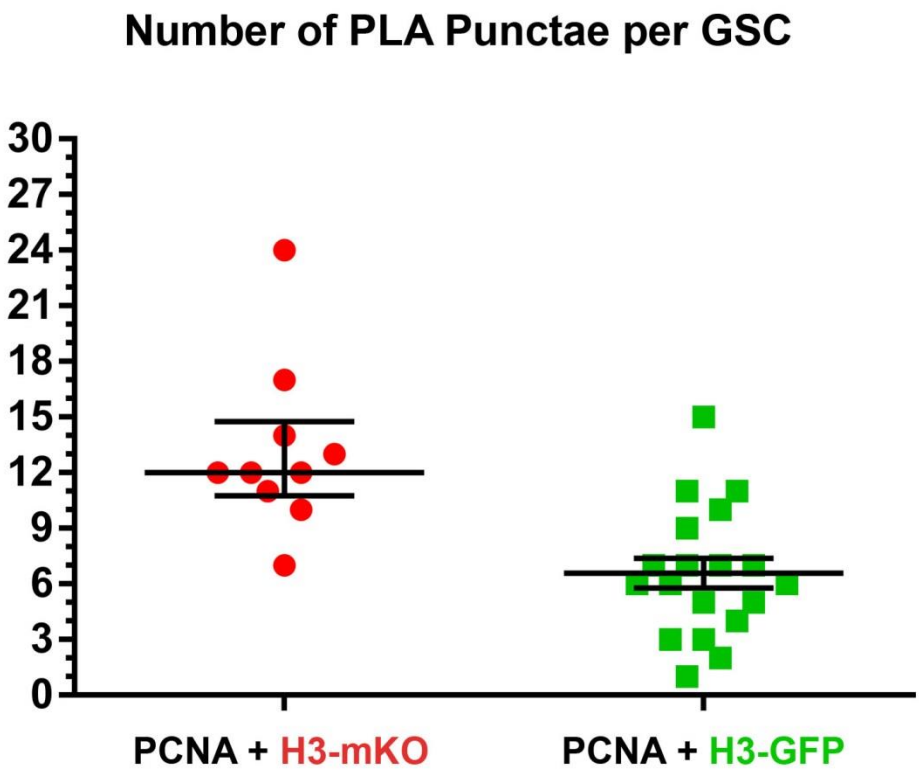

Figure S6: PLA between histones (old *versus* new) and lagging strand-enriched component PCNA. The lagging strand-enriched PCNA showed more PLA fluorescent spots with new H3 (mKO, 13.2 ± 1.4, avg. ± s.e., n = 13) than with old H3 (GFP, 6.5 ± 0.8, n = 22), $P < 0.01$, based on Kruskal-Wallis multiple comparisons of non-parametric data with Dunn's multiple comparisons corrections test.

Supplementary Movies:

Movie S1: Time-lapse imaging of the histone H4-EGFP (old) in *Drosophila* male GSC. This video is a 3D reconstruction of images (14 × 1-μm interval optical sections per frame), showing asymmetric old histone H4 segregation during asymmetric GSC division. The video was acquired at 2-min intervals and the quantification was shown in Figure 1G.

Movie S2: Time-lapse imaging of the histone H4-mCherry (new) in *Drosophila* male GSC. This video is a 3D reconstruction of images (14 × 1- μm interval optical sections per frame), showing symmetric new histone H4 segregation during asymmetric GSC division. The video was acquired at 2-min intervals and the quantification was shown in Figure 1G.

Movie S3: Time-lapse imaging of the histone H4-EGFP (old) in *Drosophila* male SG. This video is a 3D reconstruction of images (8 × 1- μm interval optical sections per frame), showing symmetric old histone H4 segregation during symmetric SG division. The video was acquired at 2-min intervals and the quantification was shown in Figure 1G.

Movie S4: Time-lapse imaging of the histone H4-mCherry (new) in *Drosophila* male SG. This video is a 3D reconstruction of images (8 × 1- μm interval optical sections per frame), showing symmetric new histone H4 segregation during symmetric SG division. The video was acquired at 2-min intervals and the quantification was shown in Figure 1G.

Movie S5: Time-lapse imaging of the histone H2A-EGFP (old) in *Drosophila* male GSC. This video is a 3D reconstruction of images (9 × 1- μm interval optical sections per frame), showing symmetric old histone H4 segregation during asymmetric GSC division. The video was acquired at 2-min intervals and the quantification was shown in Figure 2G.

Movie S6: Time-lapse imaging of the histone H2A-mCherry (new) in *Drosophila* male GSC. This video is a 3D reconstruction of images (9 × 1- μm interval optical sections per frame),

showing symmetric new histone H4 segregation during asymmetric GSC division. The video was acquired at 2-min intervals and the quantification was shown in Figure 2G.

Supplementary Tables:

Table S1: Quantification of histone H4 with imaging on fixed samples.

Pair #	Old H4 GSC/GB	New H4 GB/GSC	Pair #	Old H4 SG1/SG2	New H4 SG2/SG1
1	3.95	0.58	1	1.01	0.92
2	3.22	1.89	2	1.03	0.93
3	3.04	0.859	3	0.85	0.82
4	2.95	0.98	4	1.05	1.17
5	3.41	1.23	5	1.03	0.83
6	5.7	1.05	6	1.31	0.77
7	4.86	1.19	7	0.76	1.05
8	2.445	1.21	8	1.03	1.22
9	1.01	1.43	9	1.069	0.98
10	3.15	1.038	10	0.92	0.84
11	4.84	0.72	11	1.038	1.05
12	5.66	0.752	12	0.89	1.22
13	3.21	1.75	13	1.026	0.98
14	4.38	0.66	14	0.76	0.84
15	5.66	1.14	15	1.04	1.05
16	3.21	0.887	16	0.925	0.94
17	4.38	1.75	17	1.02	0.82
18	1.12	0.69	18	0.76	0.95
19	4.31	1.15	19	1.04	0.872
20	3.65	1.14	20	0.925	1.202
21	0.9	0.78	21	1.02	1.147
22	0.76	0.57	22	1.016	0.8
23	3.64	1.17	23	0.99	1.12
24	3.822	0.57	24	1.00	1.03
25	1.337	1.17	25	1.02	0.68
26	4.53	1.05	26	1.123	1.38
27	2.92	1.077	27	1.01	0.93
28	3.08	1.03			
29	0.94	1.287			
30	4.87	1.149			
31	5.97	2.116			
32	1.39	0.815			
33	0.98	0.982			

Table S2: Quantification of histone H4 with live imaging.

Pair #	Old H4 GSC/GB	New H4 GB/GSC	Pair #	Old H4 SG1/SG2	New H4 SG2/SG1
1	1.538655711	0.934736882	1	1.000498163	0.822924487
2	1.82913343	1.175082157	2	1.022234515	0.857135762
3	1.915116858	0.808769217	3	1.022455355	0.832345521
4	2.076755474	1.970780936	4	1.047347585	1.025446515
5	1.594852825	1.529462202	5	1.058688768	1.073933167
6	1.796000508	1.085765884	6	1.099938037	0.864781839
7	1.644972359	1.093039339	7	1.097272701	0.838004583
8	1.501172449	0.712606285	8	1.028042754	0.955042856
9	1.578491674	0.887661884	9	1.166526823	1.031956461
10	1.556435054	1.055190708	10	1.182394548	0.757649498
11	1.514881821	1.304719792	11	1.083779331	1.169209039
12	1.47880636	1.002065631	12	1.144309561	0.85589439
13	1.947659779	0.842068593	13	1.118147974	0.847057843
14	2.227387093	0.989487571	14	1.061918924	0.839005066
15	1.882287735	1.351714794	15	1.020578569	0.941319995
16	2.04907088	0.949273341	16	1.128962372	0.991380411
17	2.216802168	0.675787593	17	1.010467672	1.028997304
18	2.154094547	0.826733448	18	1.156439305	1.0535661
19	1.567278145	1.074367768	19	1.197441645	0.971507172
20	1.501715615	0.996020101	20	1.150132669	0.876660802
21	2.873081982	0.7698258	21	1.10947257	0.916218757
22	1.53534459	1.047276662	22	1.012961559	0.870208701
23	1.627815051	0.89787179	23	1.108858792	0.937771642
24	1.598326439	1.160867045			
25	1.469595531	1.006567961			

Table S3: Quantification of histone H2A with imaging on fixed samples.

Pair #	Old H2A GSC/GB	New H2A GB/GSC	Pair #	Old H2A SG1/SG2	New H2A SG2/SG1
1	0.975257657	0.98053122	1	1.088526265	1.043770558
2	0.968836869	0.966059723	2	1.016521777	1.016185595
3	0.969108816	0.941793393	3	0.94226273	0.974142098
4	1.232283465	1.633217284	4	1.067556671	0.915380396
5	1.025846378	1.041755268	5	1.009897937	0.962468942
6	1.053258093	0.999096786	6	1.042815974	0.946732867
7	0.96981108	1.186201719	7	1.019320953	0.950287833
8	0.797679181	1.357976654	8	1.222330968	0.885426578
9	1.075991617	1.122733612	9	0.995727661	1.019966875
10	1.121519519	0.901016184	10	0.930194711	1.009292519
11	1.061309268	1.103250478	11	0.931785196	0.931550686
12	0.91240285	1.066446402	12	0.986123708	0.979875209
13	0.801834862	1.204483553	13	0.925085483	1.045018182
14	1.070005651	0.987937274	14	1.019632679	1.10359635
15	0.72144534	1.247089104	15	1.035048915	1.119932432
16	1.338405425	1.246516489	16	0.969548629	0.972565036
17	0.898969072	1.154507556	17	0.972673954	1.035350772
18	1.152941753	1.019673558	18	1.023154848	1.16412729
19	1.054371002	0.823608964	19	0.978854429	1.153198983
20	0.920813893	1.027300496	20	1.055423123	1.029364311

Table S4: Quantification of histone H2A with live imaging.

Pair #	Old H2A GSC/GB	New H2A GB/GSC	Pair #	Old H2A SG1/SG2	New H2A SG2/SG1
1	0.962350834	1.397385579	1	1.096485599	0.818410393
2	1.149904299	0.813066811	2	1.190294037	0.987425561
3	1.056483442	0.897416334	3	1.011960361	0.811158596
4	1.38031258	0.766107928	4	1.031401962	0.799000521
5	1.067251462	0.938143326	5	1.15704388	0.787275176
6	1.41021415	0.882631518	6	1.111187141	0.859652969
7	1.276493273	0.759832685	7	1.0893243	0.888064467
8	1.365344872	0.848354643	8	1.107798005	0.885252984
9	1.222507353	1.211761642	9	1.095078584	0.940026255
10	1.399275942	0.840726914	10	1.175623048	0.874913478
11	1.384687264	0.764841829	11	1.16613775	1.004767174
				1.12589198	0.924295887
				1.0720282	0.975484231
				1.112568529	0.941780555
				1.095228729	0.973672302
				1.170123228	0.978181076
				1.133160858	0.977616472
				1.129348713	0.794312427
				1.062893839	0.976184067
				1.043153049	0.777470958
				1.128981038	0.840689167

Table S5: Quantification of histone H2B with imaging on fixed samples.

Pair #	Old H2B GSC/GB	New H2B GB/GSC	Pair #	Old H2B SG1/SG2	New H2B SG2/SG1
1	0.815283172	1.149883726	1	1.06879687	1.036802671
2	0.910809049	1.087101455	2	0.83419399	1.01759456
3	0.992565434	0.900208136	3	1.010622669	0.861117493
4	0.978807685	1.061501775	4	1.046838138	1.052032321
5	1.17406494	0.821823967	5	0.916185819	0.874832476
6	0.872269007	1.360653409	6	0.973981549	1.326719124
7	1.162729831	0.827364081	7	1.220158888	0.749905276
8	1.171490593	1.601112878	8	1.009274627	0.968346435
9	1.037883808	0.917360074	9	0.947504382	1.170238975
10	0.99783673	0.923628319	10	0.854147825	1.174910873
11	0.895076097	1.281920327	11	1.172142501	0.858156863
12	0.959500446	1.479566305	12	1.083404453	0.845157357
13	1.231086253	1.127473807	13	1.07626037	0.923235726
14	0.808704809	1.211914894	14	1.021646558	0.920400153
15	1.046689113	1.143965517	15	0.86262317	1.172370089
16	0.849082443	1.453828829	16	1.026491198	1.939485628
17	1.055365474	1.121270452	17	1.0234375	0.972416813
18	1.014446228	1.165391969	18	0.928342031	0.856763926
19	0.912596963	1.306268241	19	0.900293686	1.918833044
20	1.021970333	0.862912736	20	1.066753078	1.144069104
21	1.202621287	1.191425723	21	1.099325769	0.662652053
22	0.887726959	2.07110666	22	1.153474545	0.59781155
23	0.990796476	0.885693395	23	0.982679645	1.374321095
24	0.918245383	0.891502847	24	0.844495944	1.205987906
25	0.912221729	1.384310526	25	1.036036036	0.852305896
26	0.869454545	1.11416998	26	1.064761181	0.948237664
27	1.190698579	1.019536742	27	0.88406336	1.059149083
28	0.891282778	1.129701061	28	1.093008455	0.998295745
29	1.048793662	0.94980315	29	1.080438985	1.300522734
30	1.214413768	0.848577475	30	1.222637781	1.0442979
31	0.935564854	1.327795976	31	1.037889226	1.10251344
32	0.843987298	1.593786228	32	1.126153435	0.977582529
33	1.011382114	1.166823456	33	0.813552882	0.91765286
34	0.907251972	1.466248278	34	1.083184342	0.968471789
35	0.894008235	1.033427164	35	0.904325323	1.031899183
36	1.110156314	1.905524681	36	1.015971606	1.013173653
37	0.917364991	1.476244026			

38	0.964285714	1.280842528			
39	0.976632851	2.048527984			
40	0.96929659	0.890530557			

Table S6: Information for Figure S2.

	Spot density of Dronpa (μm^{-2})	Spot density of PAmCherry (μm^{-2})
H3	79 ± 44[a]	38 ± 34
H3.3	78 ± 67	42 ± 17

	Nyquist of Dronpa (nm)[b]	Spot density of PAmCherry (nm)
H3	225 ± 62	323 ± 114
H3.3	226 ± 98	309 ± 62

a. Standard Deviation (N = 36 and 38 respectively).

b. 2D-Nyquist sampling resolution was calculated based on $R = \frac{2}{\sqrt{D}}$, where D is the spot density (Jones et al., 2011).

Supplementary References:

Buss, J., Coltharp, C., Shtengel, G., Yang, X., Hess, H., and Xiao, J. (2015). A multi-layered protein network stabilizes the Escherichia coli FtsZ-ring and modulates constriction dynamics. PLoS Genet *11*, e1005128.
Coltharp, C., Buss, J., Plumer, T.M., and Xiao, J. (2016). Defining the rate-limiting processes of bacterial cytokinesis. Proc Natl Acad Sci U S A *113*, E1044-1053.
Coltharp, C., Yang, X., and Xiao, J. (2014). Quantitative analysis of single-molecule superresolution images. Curr Opin Struct Biol *28*, 112-121.
Dempsey, G.T., Vaughan, J.C., Chen, K.H., Bates, M., and Zhuang, X. (2011). Evaluation of fluorophores for optimal performance in localization-based super-resolution imaging. Nat Methods *8*, 1027-1036.
Hensel, Z., Weng, X., Lagda, A.C., and Xiao, J. (2013). Transcription-factor-mediated DNA looping probed by high-resolution, single-molecule imaging in live E. coli cells. PLoS Biol *11*, e1001591.
Hime, G.R., Brill, J.A., and Fuller, M.T. (1996). Assembly of ring canals in the male germ line from structural components of the contractile ring. J Cell Sci *109 (Pt 12)*, 2779-2788.
Hoogendoorn, E., Crosby, K.C., Leyton-Puig, D., Breedijk, R.M., Jalink, K., Gadella, T.W., and Postma, M. (2014). The fidelity of stochastic single-molecule super-resolution reconstructions critically depends upon robust background estimation. Sci Rep *4*, 3854.
Jones, S.A., Shim, S.H., He, J., and Zhuang, X. (2011). Fast, three-dimensional super-resolution imaging of live cells. Nat Methods *8*, 499-508.
Ovesny, M., Krizek, P., Borkovec, J., Svindrych, Z., and Hagen, G.M. (2014). ThunderSTORM: a comprehensive ImageJ plug-in for PALM and STORM data analysis and super-resolution imaging. Bioinformatics *30*, 2389-2390.
Tran, V., Lim, C., Xie, J., and Chen, X. (2012). Asymmetric division of Drosophila male germline stem cell shows asymmetric histone distribution. Science *338*, 679-682.
Van Doren, M., Williamson, A.L., and Lehmann, R. (1998). Regulation of zygotic gene expression in Drosophila primordial germ cells. Curr Biol *8*, 243-246.
Veatch, S.L., Machta, B.B., Shelby, S.A., Chiang, E.N., Holowka, D.A., and Baird, B.A. (2012). Correlation functions quantify super-resolution images and estimate apparent clustering due to over-counting. PLoS One *7*, e31457.